Team Structure

[1]Eyob Ghebreiesus [2]James Szewczyk [3]Marek Jelen [4]Matt Tobin

[1] M.Eng. Aerospace Engineering. Aerodynamics Lead. Deputy for Stability Control.
[2] B.Sc. Aerospace Engineering. Propulsion Lead, Deputy for Structures
[3] M.Eng. Aerospace Engineering. Stability Control Lead, Deputy for Aerodynamics
[4] M.Sc. Aerospace. Structures Lead, Deputy for Propulsion.

Homepage: *Project Morbius*
Created on *October* 25^{th}*, 2022*
Published on *December* 1^{st}*, 2022*

Produced via LaTeX, Inc U.S.A.
MIT License for the GitHub Project, 2022
github.com/eyobghiday/project-morbius

Department of Mechanical, Materials and Aerospace Engineering
ILLINOIS INSTITUTE OF TECHNOLOGY

Contents

List of Tables

List of Figures

Abbreviations and Symbols

α	Aircraft angle of attack [deg]
AIAA	American Institute of Aeronautics and Astronautics
AR	Aspect ratio [–]
b	Wingspan [in, ft]
c	Wing chord [in]
C_d, C_D	Drag coefficient (2D, 3D) [–]
C_{D0}	Zero-lift drag coefficient
C_f	Skin friction coefficient
C_{HT}	Horizontal tail coefficient [–]
C_l, C_L	Lift coefficient (2D, 3D) [–]
$C_{L_{\max}}$	Maximum lift coefficient [–]
C_m, C_M	Moment coefficient (2D, 3D) [–]
C_{VT}	Vertical tail coefficient [–]
CA	Cyanoacrylate adhesive
CAD	Computational Aided Design
CFD	Computational fluid dynamics
CG	Center of gravity [in]
CNC	Computer numerical controlled
D	Drag
e	Oswald efficiency
ESC	Electronic speed controller
FEA	Finite element analysis
g	acceleration of gravity
IC	Integrated Circuit
IIT	Illinois Institute of Technology
LE	Leading Edge
LED	Light Emitting Diode
L	Lift
$\frac{L}{D}$	Lift-to-drag ratio [–]
NiCd	Nickel-cadmium
S_{wet}	Wetted area
TE	Trailing Edge
θ	Theta
$\frac{T}{W}$	Thrust-to-weight ratio [–]
UAV	Unmanned aerial vehicle
$\frac{W}{S}$	Wing loading [–]
W_S	Sensor pod weight [oz., lbf.]
v	Velocity [ft/s]
Wh	Watt-hours

1 Introduction

The team is made of four members in total and their roles are shown in Table 1.1. Each role has a lead and a deputy that represent their significance and the tasks delegated.

Table 1.1 – Team Organization Chart

Section	Lead	Deputy
XFLR5 Coefficients	Eyob Ghebreiesus	James Szewczyk
Climb Performance	James Szewczyk	Eyob Ghebreiesus
Glide Trajectory	Matthew Tobin	James Szewczyk
Landing Performance	James Szewczyk	Eyob Ghebreiesus
Hold Performance	Eyob Ghebreiesus	James Szewczyk
Presentation Slides	Matthew Tobin	Marek Jelen
LaTeX Report	Eyob Ghebreiesus	Matt Tobin, James Szewczyk

1.1 Project Summary

With the conceptual design of the It's Morbin Time 2022 (IMT-22) aircraft being completed, control system modelling could begin. To test this, a MATLAB Simulink model was made to control a variety of maneuvers that an aircraft would complete during a standard transportation mission. To be able to run the analysis for IMT-22, Simulink required the datum and aircraft's aerodynamic coefficients increment matrices, in addition to the aircraft's weight, center of gravity and center of pressure. These values were found from the XFLR5 model made for the aircraft in the conceptual design phase.

This report begins with discussing the values used in the XFLR5 model to compute the aerodynamic coefficients, which were needed to run the Simulink model. The report then moves on to discuss the different maneuvers the aircraft will be completing. First, the glide performance is shown to demonstrate how the aircraft will fly in the case of all engines out and the control surfaces at trimmed conditions. The aircraft's glide path can be seen and its Lift-to-Drag ratio is computed. The second maneuver is the takeoff and climb performance. The aircraft's climb rate and leveling flight variation is obtained. The third maneuver evaluated the holding pattern performance. This showed the aircraft's ability to fly a standard holding pattern with minimal altitude change. The final maneuver demonstrates exiting the pattern and preparation for landing.

1.2 XFLR5 Data and Values

The first step before creating the Simulink model is to generate the coefficient blocks of a variety deflections and roll angles, as well as getting the values required for the MATLAB Simulink. Table 1.2 shows the numbers and values needed for Simulink. Simulink's linear interpolation was used for values not discretely calculated in the XFLR simulations.

Table 1.2 – XFLR5 Values

Parameter	Value	Unit
Initial Mass	27016	kg
$[X_{cog}, Y_{cog}, Z_{cog}]$	$[-0.886, 0, -0.631]$	m
X_{np}	-1.862	m
Density	1.225	$\frac{kg}{m^3}$
Cruise Speed	180	$\frac{m}{s}$
MAC	2.59	m
Span	30.54	m
Ref Area	75.59	m^2

Also from XFLR, the inertia matrix used for the model of the IMT-22 is:

$$\begin{bmatrix} I_{xx} & I_{xy} & I_{xz} \\ I_{yx} & I_{yy} & I_{yz} \\ I_{zx} & I_{zy} & I_{zz} \end{bmatrix} = \begin{bmatrix} 229042 & 0 & 264144 \\ 0 & 1444714 & 0 \\ 264144 & 0 & 1531691 \end{bmatrix} \begin{bmatrix} kg.m^2 \\ kg.m^2 \\ kg.m^2 \end{bmatrix}$$

2 Coefficient Increment Graphs

Before flight simulation was able to be ran in the Simulink model, it is necessary to create matrices of both the datum and increment matrices for each of the surface deflections for the aerodynamic coefficients. The datum is a simulation of the aircraft in level flight at cruise with no control surface deflections. To begin with Figure 2.1a, 2.1b and 2.1c show the C_L, C_D, C_M graphs from the XFLR5. Notice the trim angle 3.2 deg shown in Figure 2.1.These values are plotted as a function of angle of attack. The lift, drag and moment coefficients for the datum and elevator deflection are found in Figure 2.3 respectively. The roll, pitch, and yaw deflection coefficients for beta, rudder, and aileron are found in Figures 2.2, 2.4, and 2.5, respectively. The Matlab script used to generate those plots can be found in the appendix (10) section.

For the datum value, it can be seen that C_D increases as angle of attack increases and for low angle of attack the value approaches zero. At high angles of attack, C_D increases with positive elevator deflection and vice versa. For the coefficient of lift,C_L, it increases with increasing angle of attack as well as positive elevator deflection since the elevator produces more lift. Since the aircraft is longitudinally stable, the moment coefficient, C_M, decreases with increasing angle of attack and the trim occurs at an angle of attack of 3.2 degrees.

The coefficients of roll, yaw, and pitch are C_l, C_Y, and C_n, respectively. These values are dependent on the side slip angle and aileron and rudder deflection. Positive side slip results in a negative C_l, which is needed for the aircraft's lateral stability. Also, having positive aileron deflection rolls the aircraft to the right, thus the increment for C_l from aileron deflection is positive. For C_Y, having

a positive side slip causes the aircraft to return to the trimmed condition, if it has drifted away. For C_n, it will be positive when the side slip is positive and having a positive rudder deflection will result in a negative C_Y.

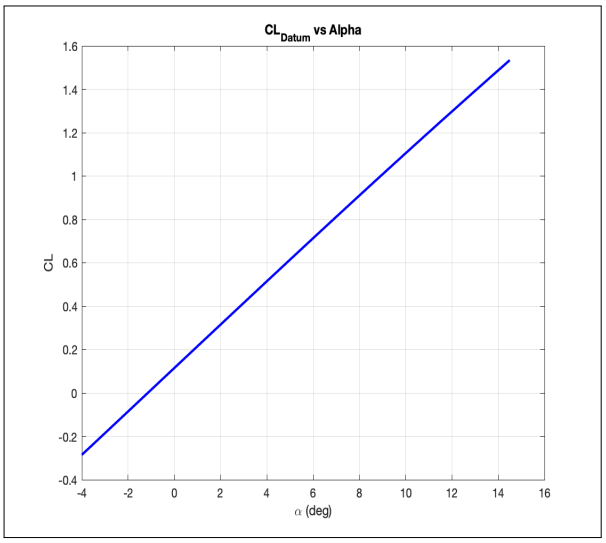

(a) C_L Datum

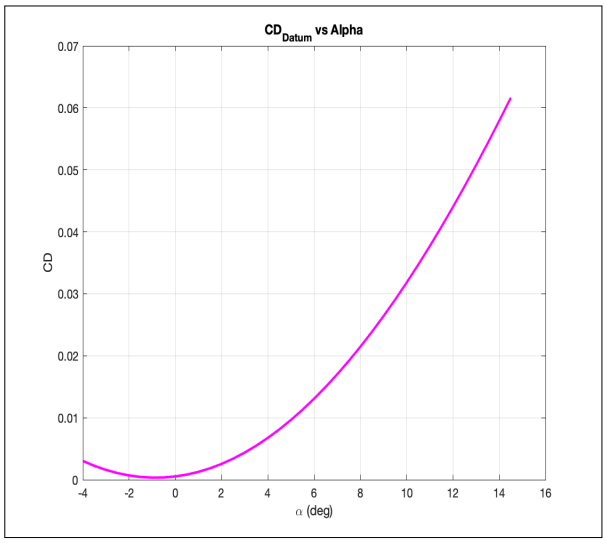

(b) C_D Datum.

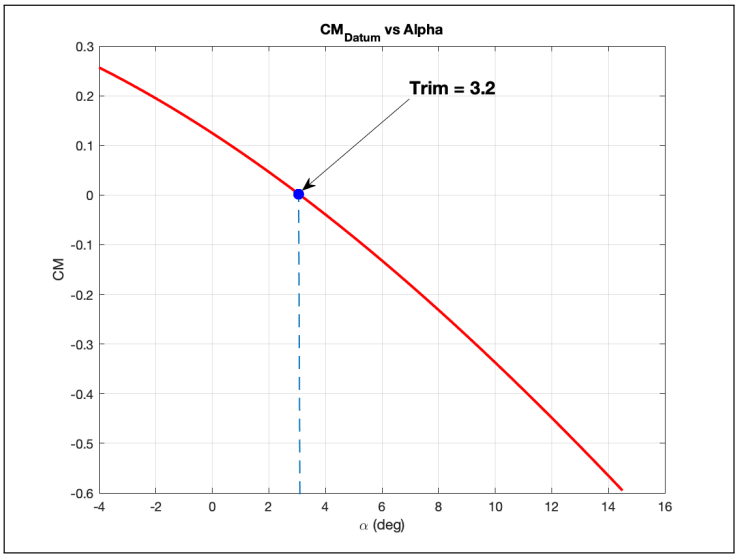

(c) C_M Datum showing Trim

Control Surface	Deflection Angle
Elevator	1
Rudder	0
Aileron	0
Flaps	0
Slats	0
Trim Angle	3.2

(d) Table of Deflection

Figure 2.1 – Airplane Datum at Trim Conditions

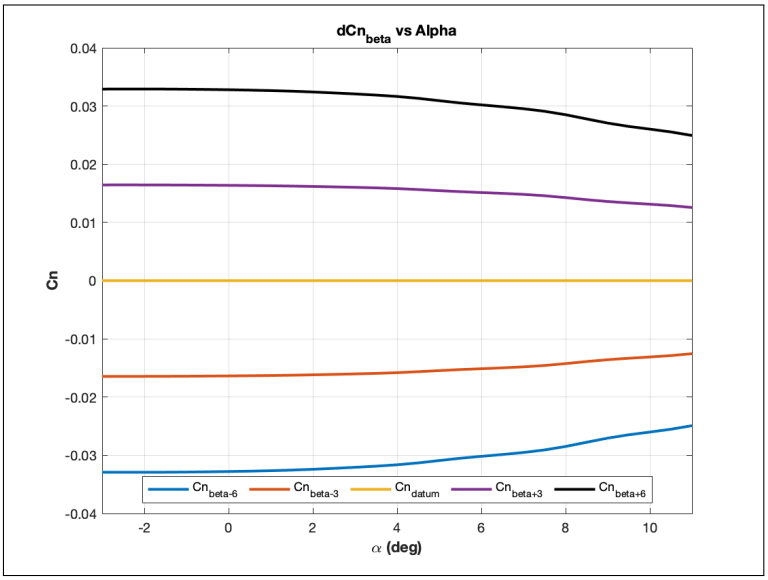

(a) dCn Beta

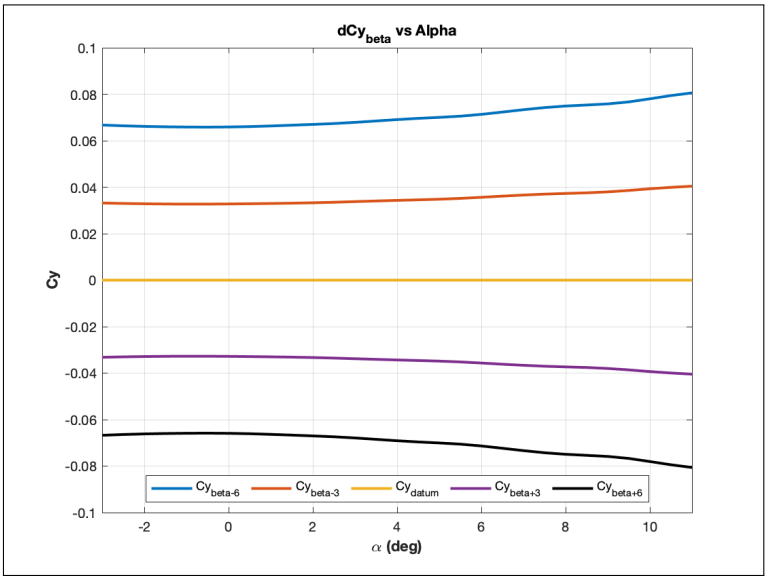

(b) dCy Beta

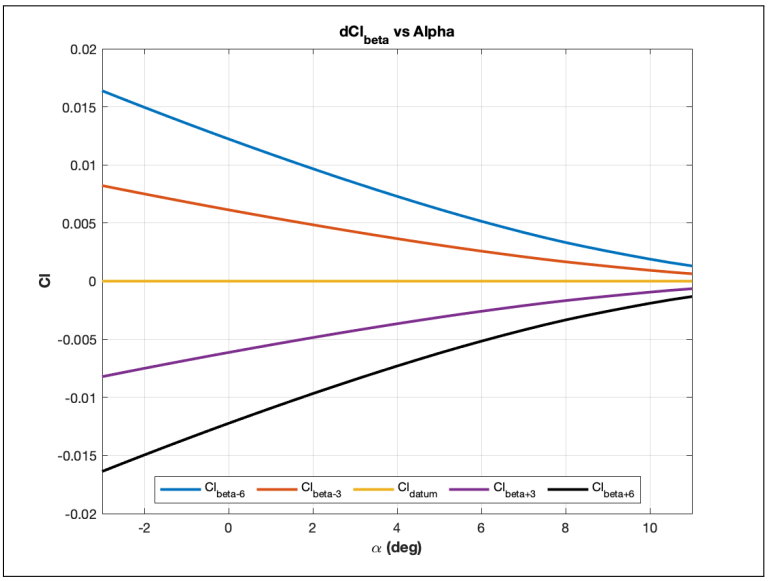

(c) dCl Beta

Figure 2.2 – dCn, dCy, dCl of Beta(Side Slip)

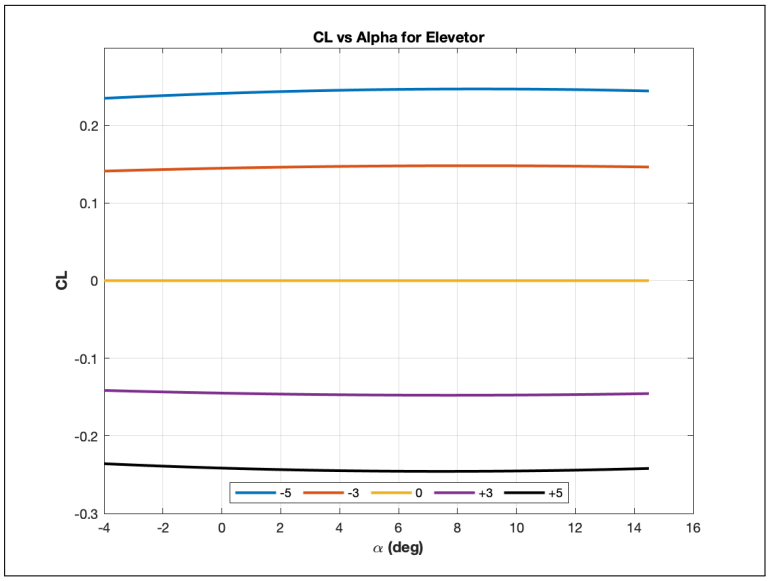

(a) C_L

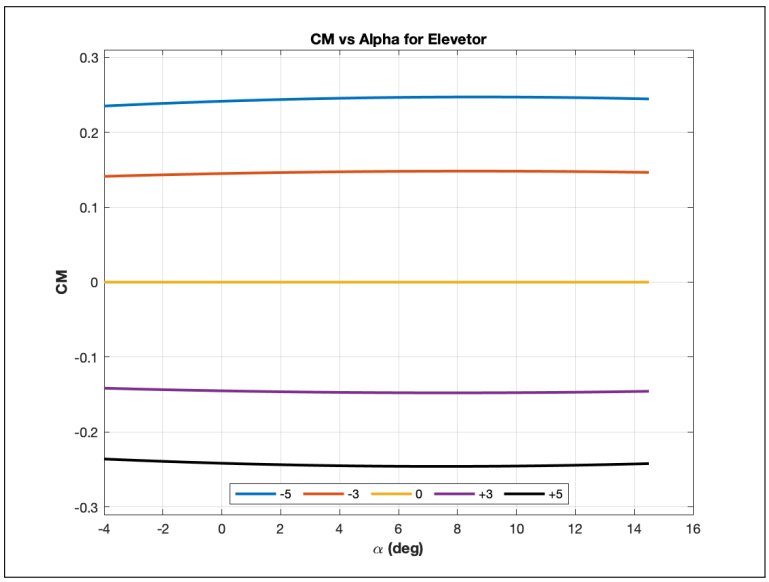

(b) C_M

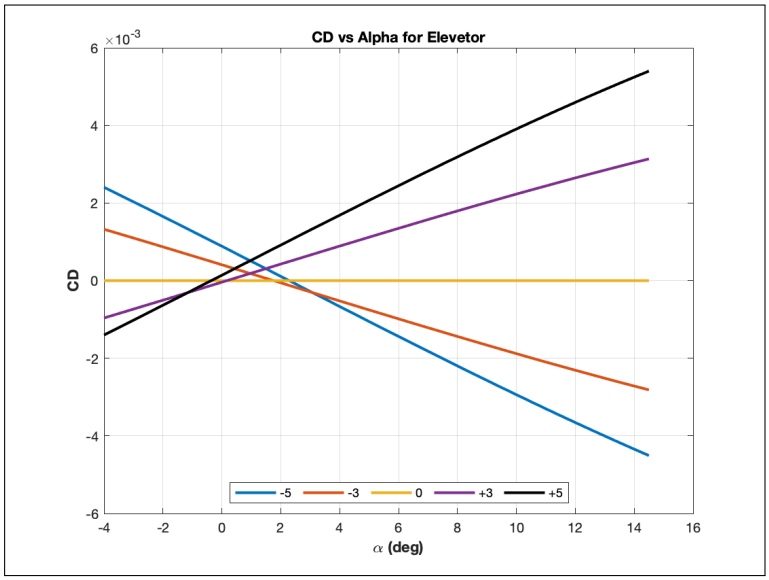

(c) C_D

Figure 2.3 – (C_L, C_M, C_D) of Elevator deflection

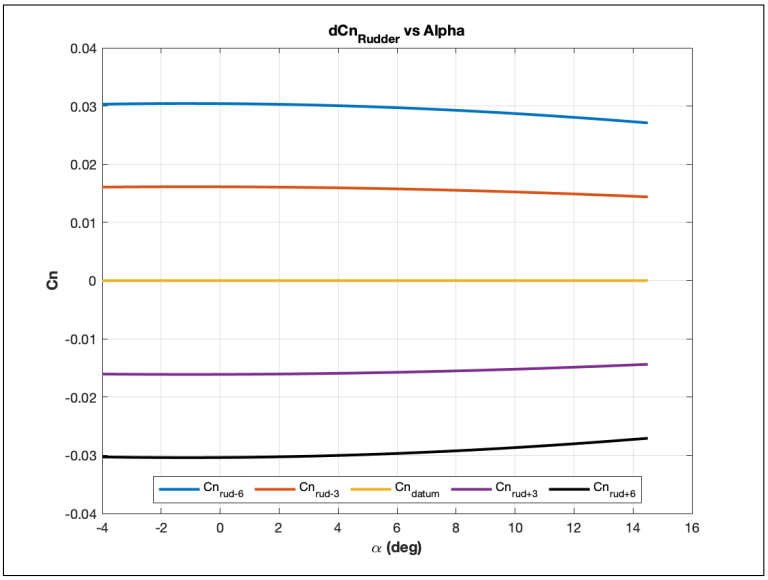

(a) dCn Rudder

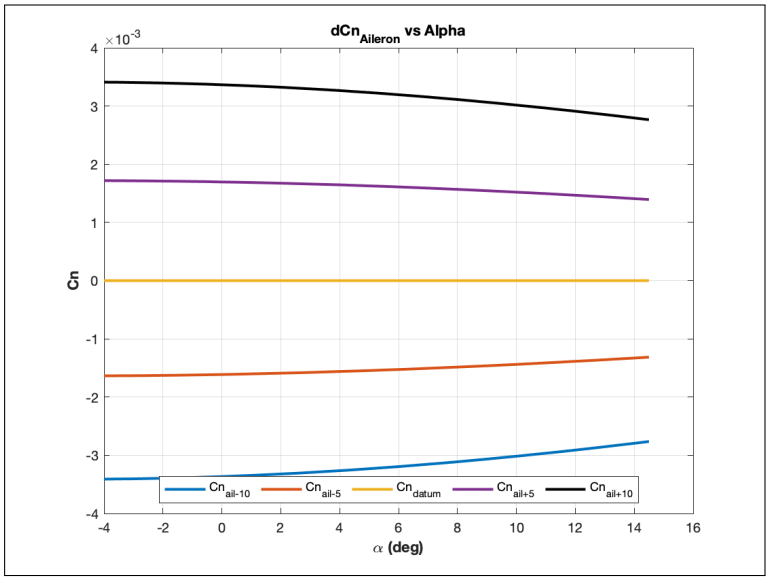

(a) dCn Aileron

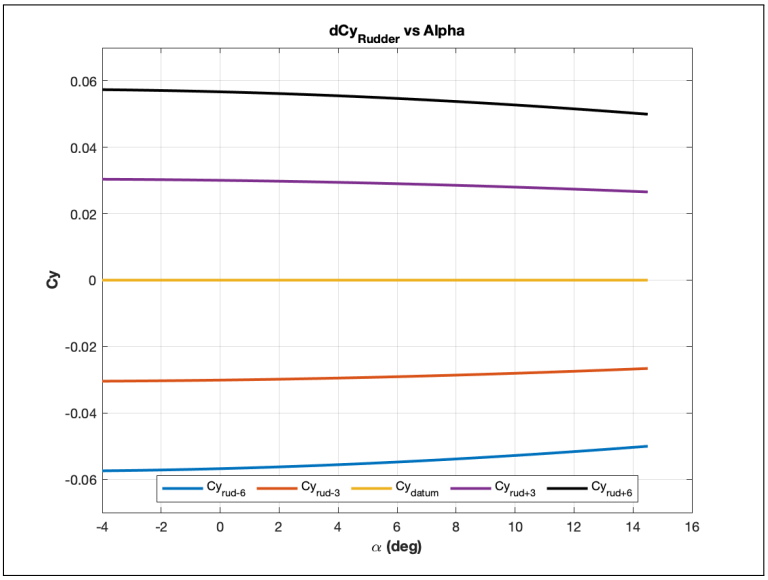

(b) dCy Rudder

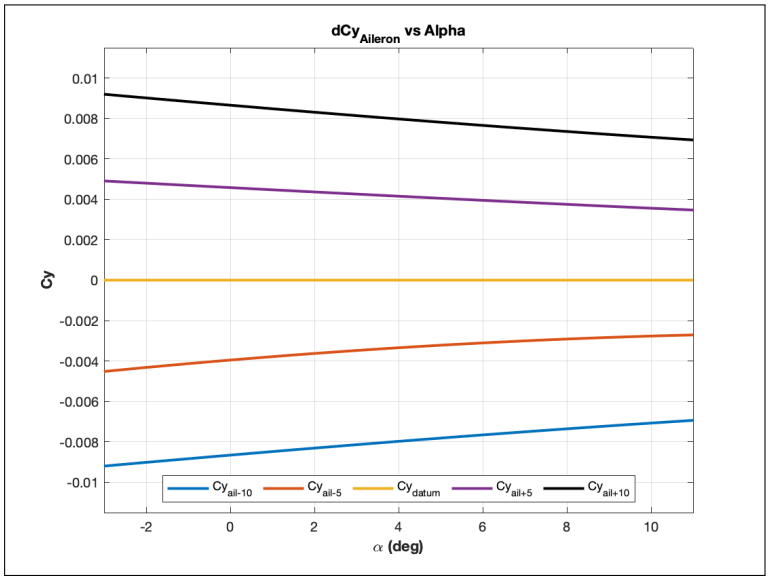

(b) dCy Aileron

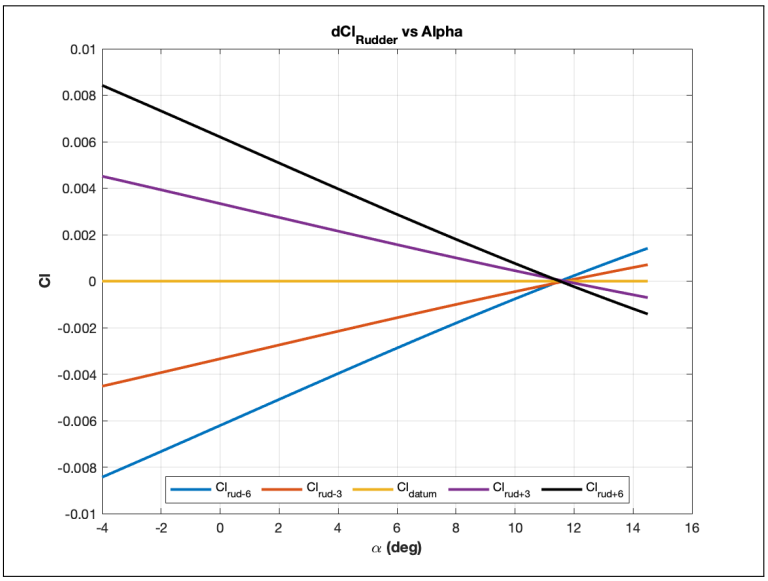

(c) dCl Rudder

Figure 2.4 – dCn, dCy, dCl of Rudder

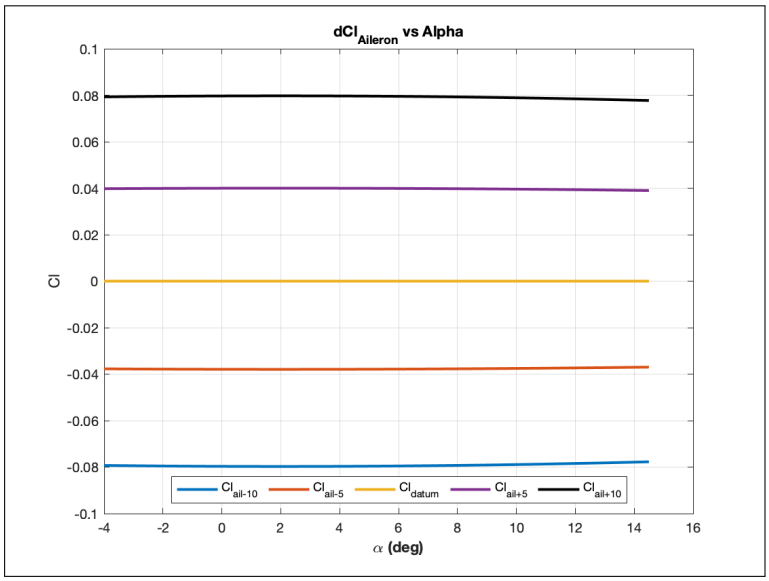

(c) dCl Aileron

Figure 2.5 – dCn, dCy, dCl of Aileron

3 Simulink Control Blocks

The full Simulink 6 degree of freedom (6DOF) model is shown in Figure 3.1 for the six-degree of freedom configuration. Not all blocks were utilized for the glide and climb tests, and a 3 degree of freedom model was used in these two tests to simplify and improve runtime.

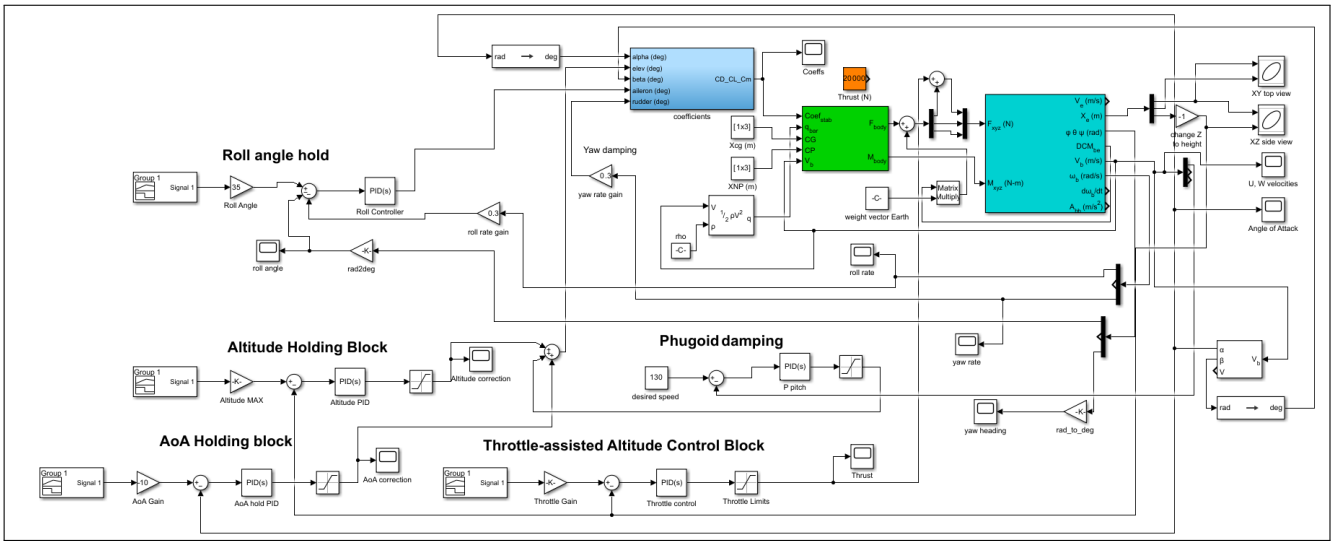

Figure 3.1 – Full Simulink Model

Each block of the control system is further zoomed in below, as well as a description of the feedback source and output signal destination. Deflection of the elevator was limited to ± 20 degrees. The throttle range in Figure 3.4 was limited to a range of 0 to 30,000 kilonewtons.

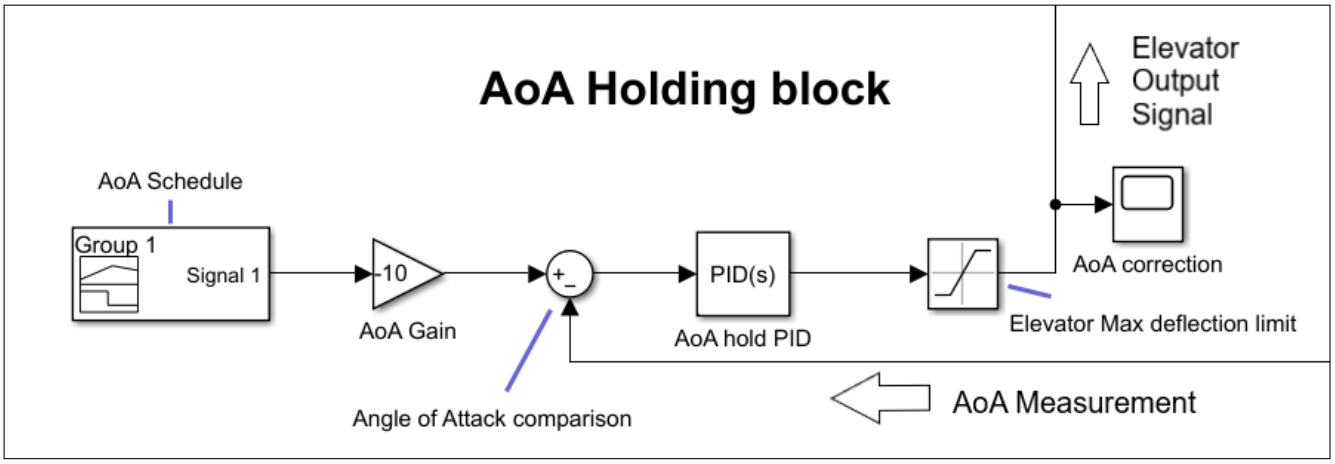

Figure 3.2 – Angle Of Attack Holding Block

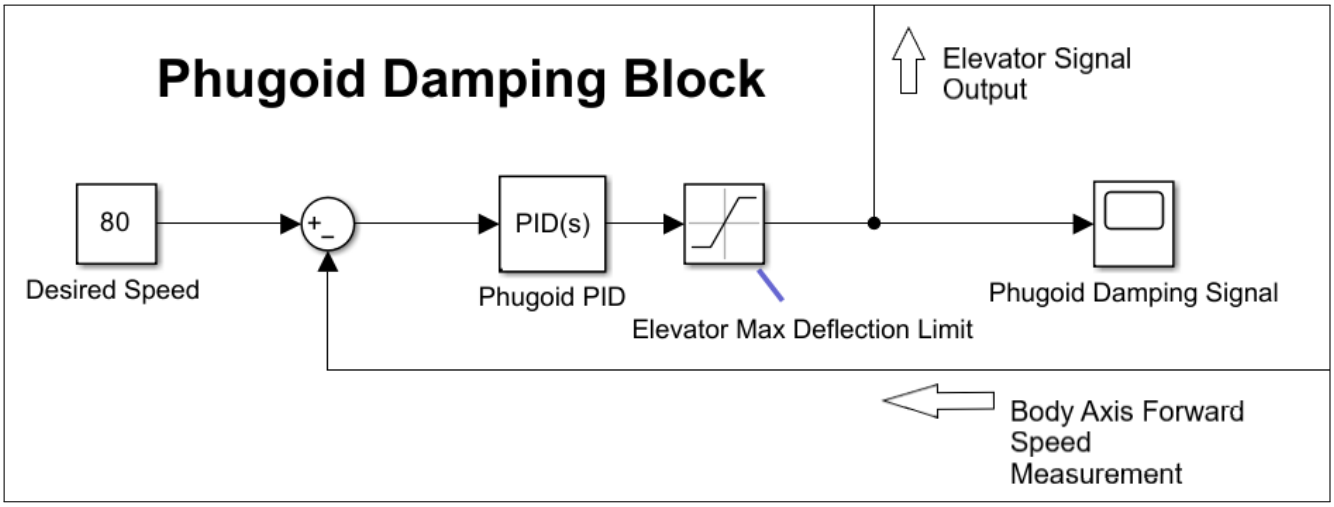

Figure 3.3 – Phugoid Damping Block

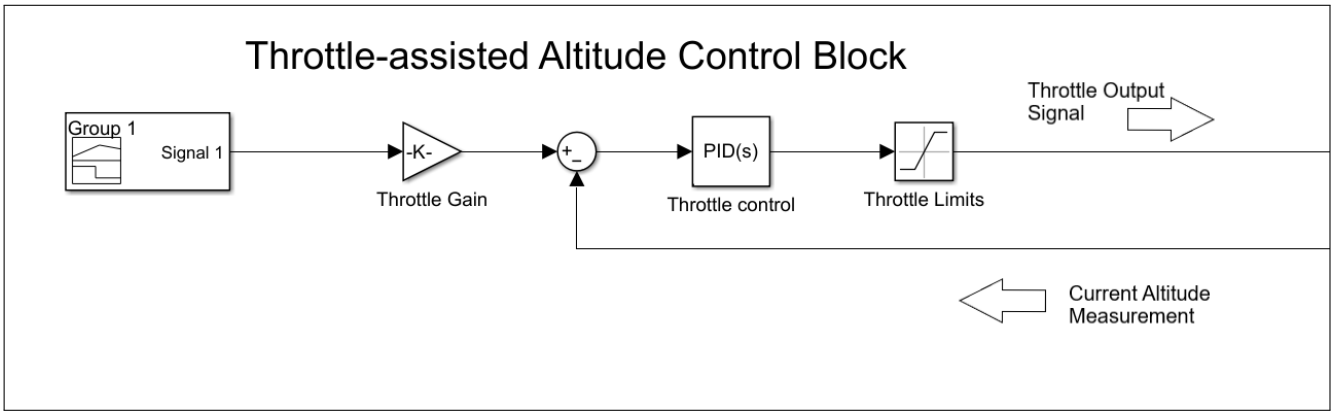

Figure 3.4 – Throttle Control Block

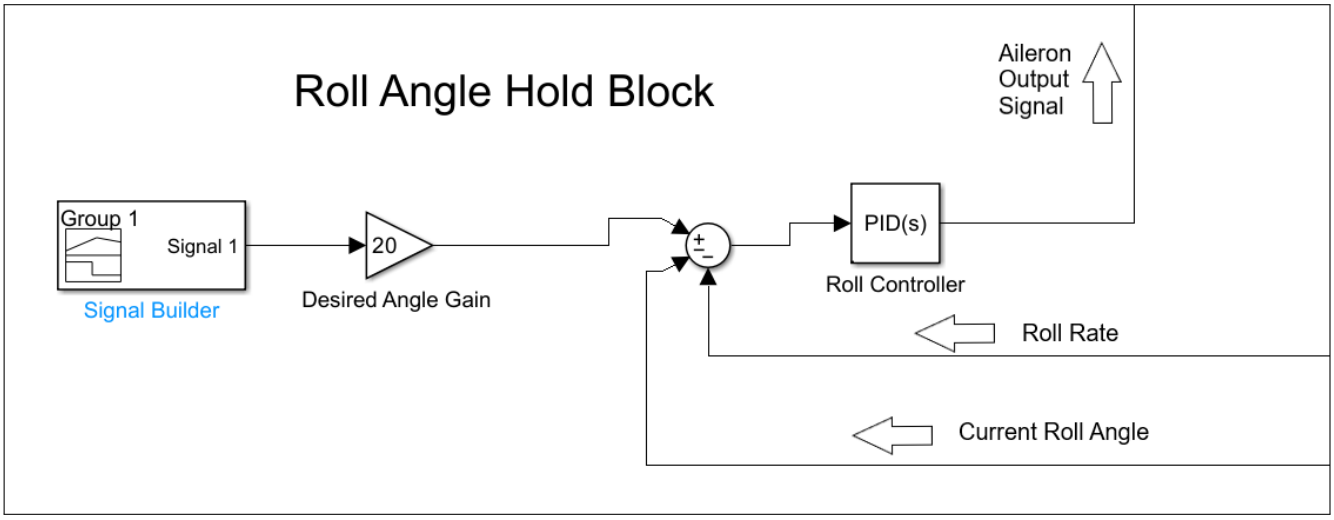

Figure 3.5 – Roll Angle Holding Block

PID Controllers were used in the blocks shown to control the aircraft during flight. The initial gains for the controllers were estimated using the Ziegler–Nichols method [8], with further adjustment

to reduce overshoot and attempt to improve settling time. I gain was not used in the throttle control due to the large instability and satisfactory performance of a PD system. Over damping was used in the altitude control systems to allow for a smooth transition to the desired altitude with no overshoot.

4 Glide Performance

The glide trajectory was found by releasing the aircraft from an altitude of 3,000 ft at its cruise speed of 180 knots with no thrust. The aircraft was trimmed and an elevator deflection of -3.23 degrees was used to damp the phugoid motion. The ailerons and rudder deflection angles were set at zero degrees as well. Figure 3.1 shows the X-Z trajectory of the glide. The aircraft lost an altitude of 3,000 ft and traveled a distance of 160,000 ft or (a glide of 32 miles) before it hit the ground. The calculated lift-to-drag ratio (L/D) of 30.1 is high for an airplane of this size, but given the higher aspect ratio and limitation of drag calculation, the actual L/D is likely lower.

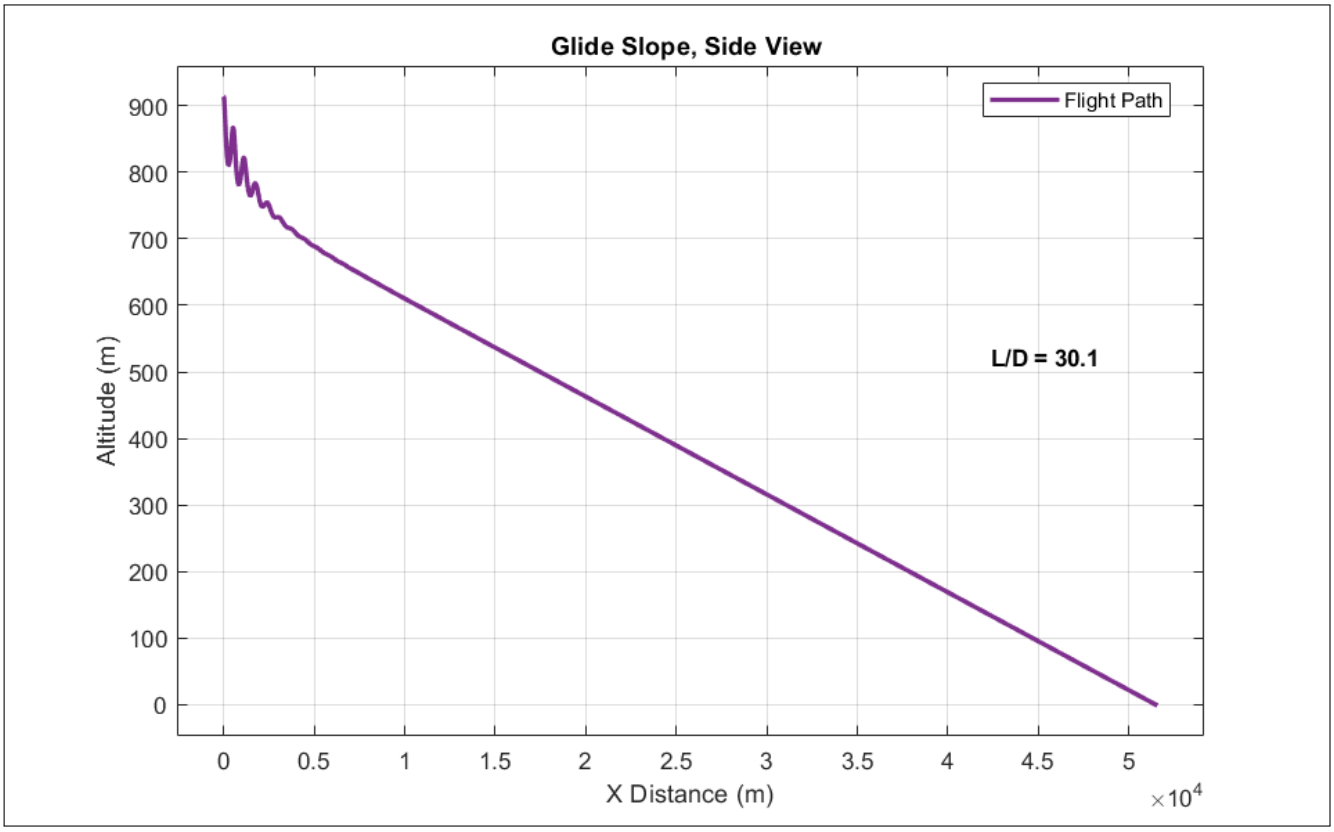

Figure 4.1 – Glide Trajectory. (X,Z) Plane

5 Takeoff and Climb Performance

For takeoff and climb, the aircraft must begin at rest at ground level, and climb to an altitude of 2500 feet above ground level (762 meters) with a climb rate greater than 600 feet per minute. The aircraft must then maintain level flight for 10 seconds afterward.

Maximum thrust was used for takeoff and climb, and reduced for cruising conditions. The maximum angle of attack experienced by the aircraft was 8 degrees shortly after takeoff, with a takeoff distance of 2378 ft (725 m) using Yechout [7] average acceleration method to find takeoff distance and time. At no point during climb did velocity drop below stall speed. Level flight was attained, with a small drop in altitude of .25 meters in the 10 seconds after leveling out.

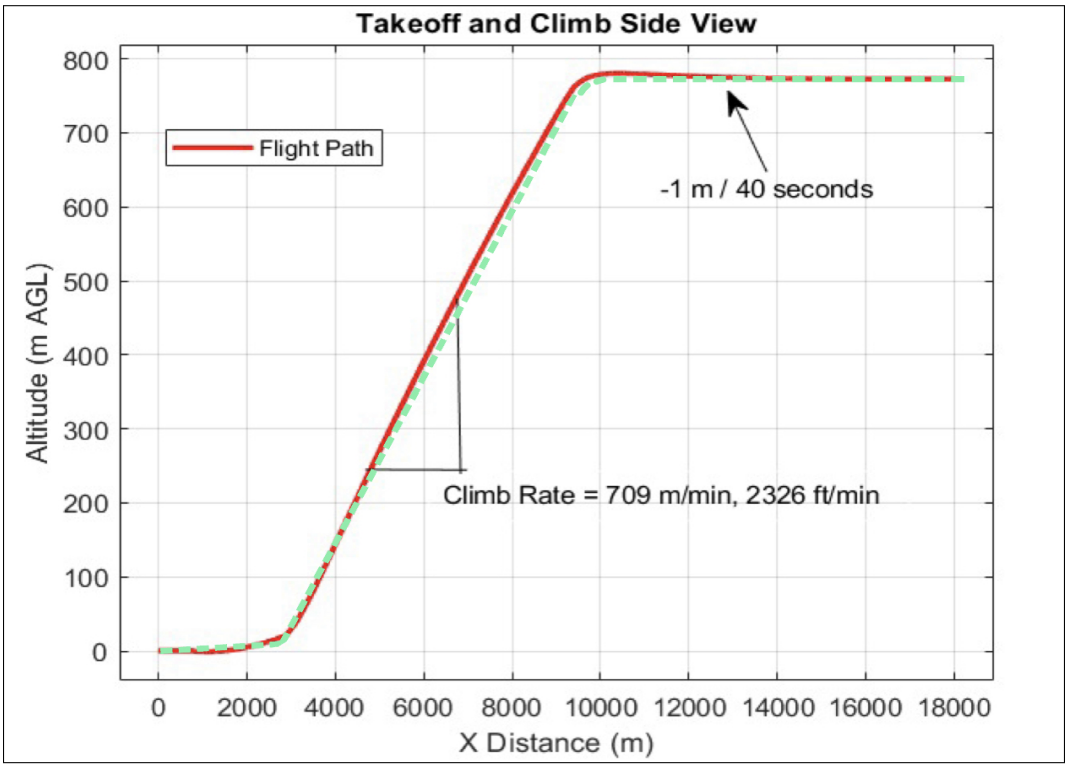

Figure 5.1 – Take off and Climb. (X,Z) Plane

The climb rate of the aircraft was 2326 feet (709 meters) per minute. This is well above the 600 ft/min requirement, but is concerning. Investigation of the velocities indicate the craft was still accelerating during climb, up to a final velocity of 230 m/s. This excess velocity is the result of using maximum thrust for climb. Additionally, this may be caused by a failure to model viscous effects, compressibilty effects, and stall prediction in this simulation. As a result of the high speed, elevator control is the dominant control method during the simulation. Further iteration would seek to more accurately model this climb prediction with a reduced throttle profile, better modelling of aerodynamic effects, and a plane speed control method.

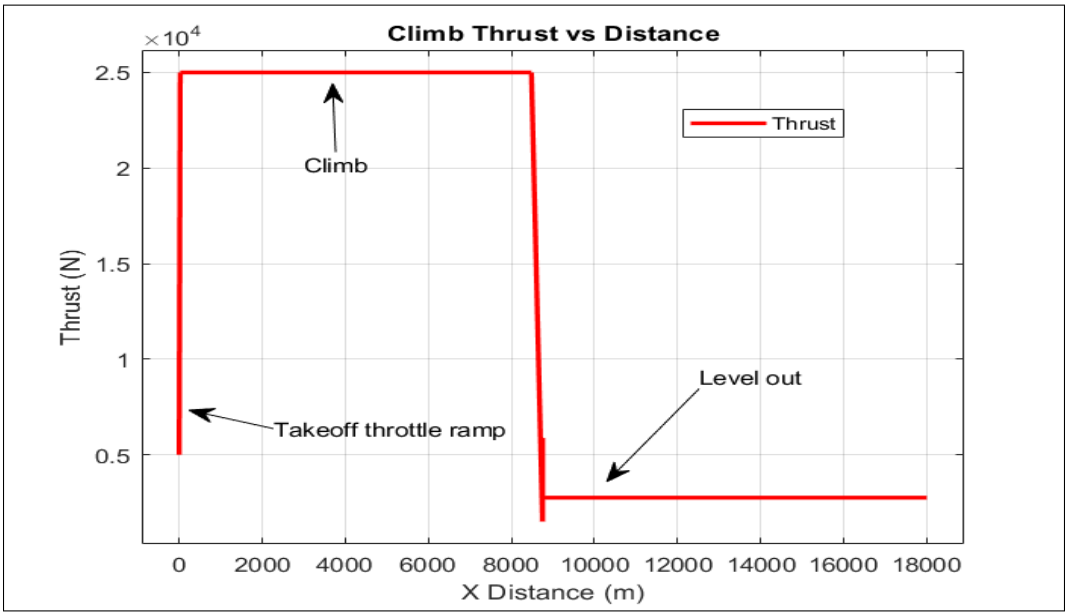

Figure 5.2 – Thrust vs X-distance for Takeoff and Climb

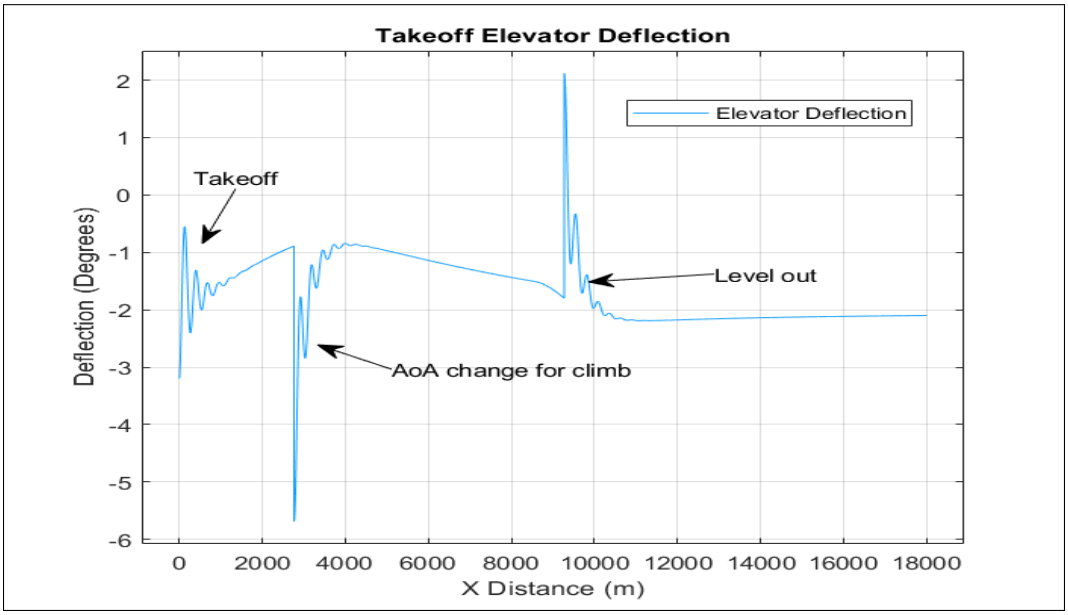

Figure 5.3 – Elevator Deflection vs X-distance for Takeoff and Climb

6 Holding Performance

The airplane is required to enter a holding pattern. The airplane uses a direct entry at 5,000 m (16,404 ft) above ground level (AGL) at a speed of approximately 253 kts (130 m/s). After flying for 1 minute, the plane makes a left turn at 3 deg/sec for 1 minute so that it is flying at 180 degrees from the original heading. The plane flies on this heading for 1 minute, then begins another 3 deg/sec left turn for 1 minute. The plane then is back on the inbound leg to the holding fix.

The results of the desired and actual (x,y) trajectory is shown in Figure 6.1. The bank angle used was 25 degrees. After damping the phugoid motion during the entry, the height of the aircraft during the pattern varies by approximately ± 12 meters (40 ft) see Figure 6.2. The distance between the inbound and outbound leg is approximately 6.32 miles. This can be reduced by increasing the bank angle and / or lowering the speed of the aircraft.

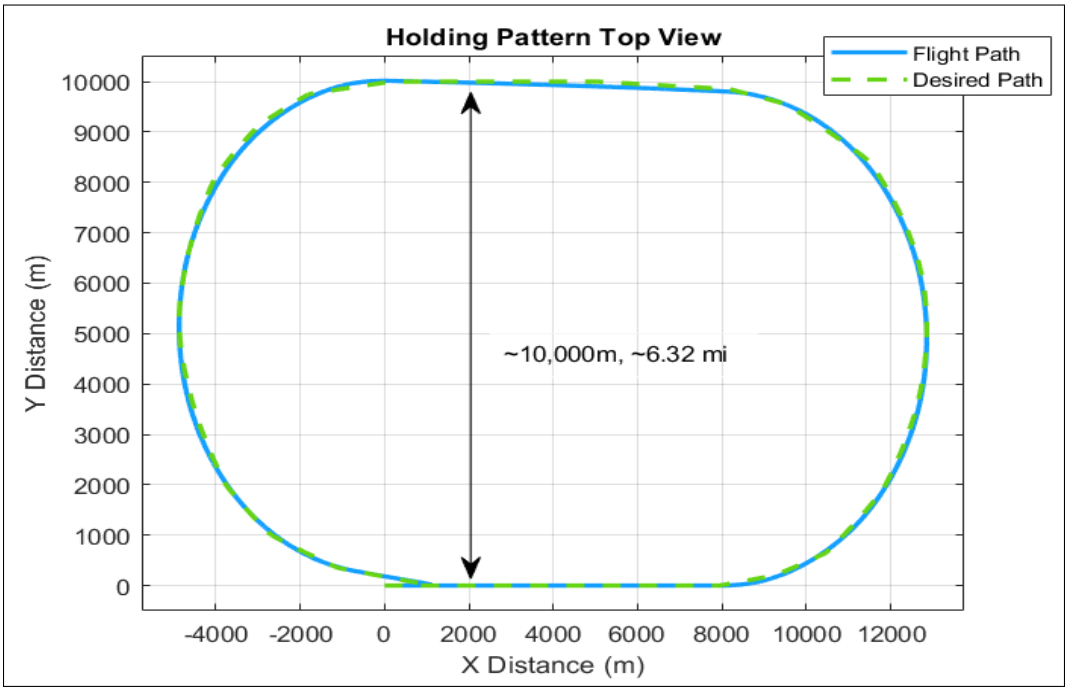

Figure 6.1 – Hold Top View. (X,Y) Plane

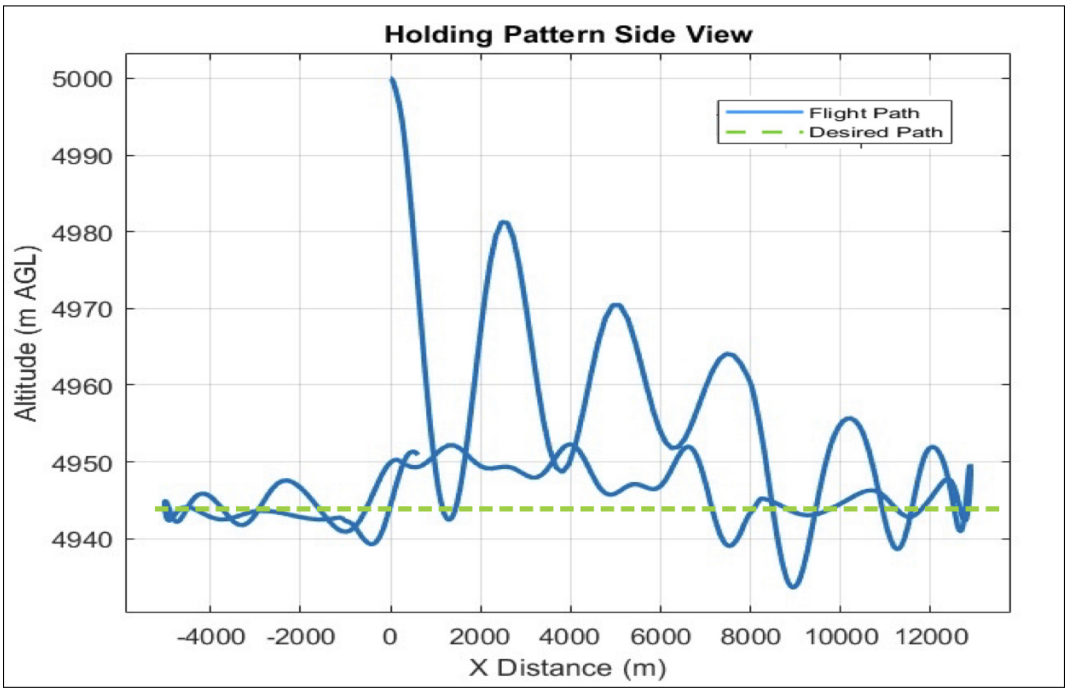

Figure 6.2 – Hold Side View. (X,Z) Altitude Plane

7 Landing Performance

For the first 25 seconds, the airplane enters the downwind leg of a left-hand landing pattern at 45 deg and an altitude of 1000 ft (305 m) AGL at a speed of 80 m/s (155 knots). The airplane then makes a 45 deg right turn to fly the downwind leg. It was then slowed down to an approach speed of 60 m/s (116.6 knots) in order to descend to 600 ft AGL on the downwind leg. Figure 7.1 shows the commanded and actual top view (x,y) flight trajectory. The airplane then makes a 90 deg left turn to fly the base leg. The airplane makes another left turn, which is aligned with the runway for its final approach maintaining its altitude and speed during the turn.

Figure 7.2 is the actual altitude trajectory (x,z) plot in comparison with the desired altitude trajectory. The distance between the downwind leg final landing is approximately 8 miles. This distance can be shortened via pilot control, and the long distance is a symptom of the overdamped altitude control, implemented to prevent ground strikes [7]. Figure 7.3 shows the roll angles commanded during landing. The targeted bank angle was 35 degrees. Thrust was varied during landing with a signal builder and PD controller to reduce thrust for landing after executing the turns. Thrust on final approach was reduced to zero for landing.

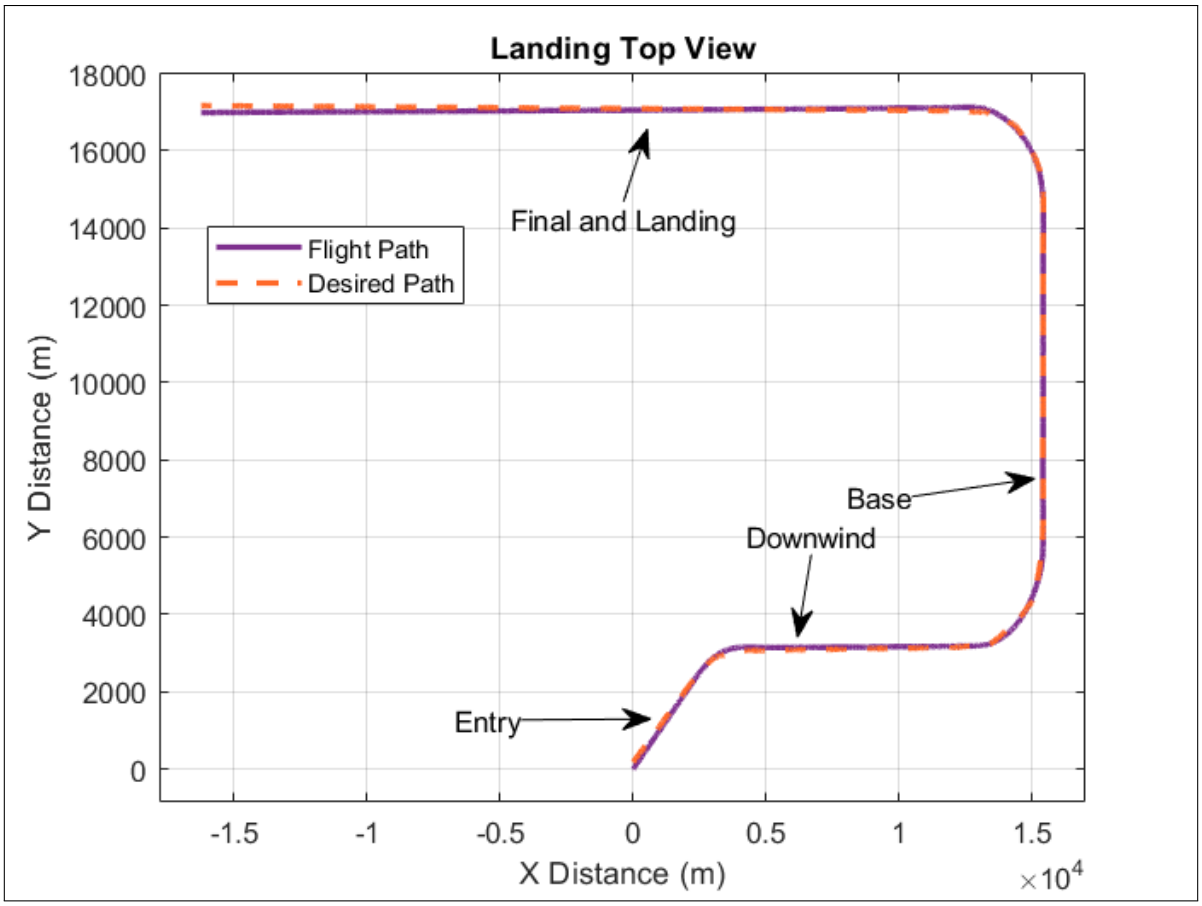

Figure 7.1 – Landing Top View. (X,Y) Plane

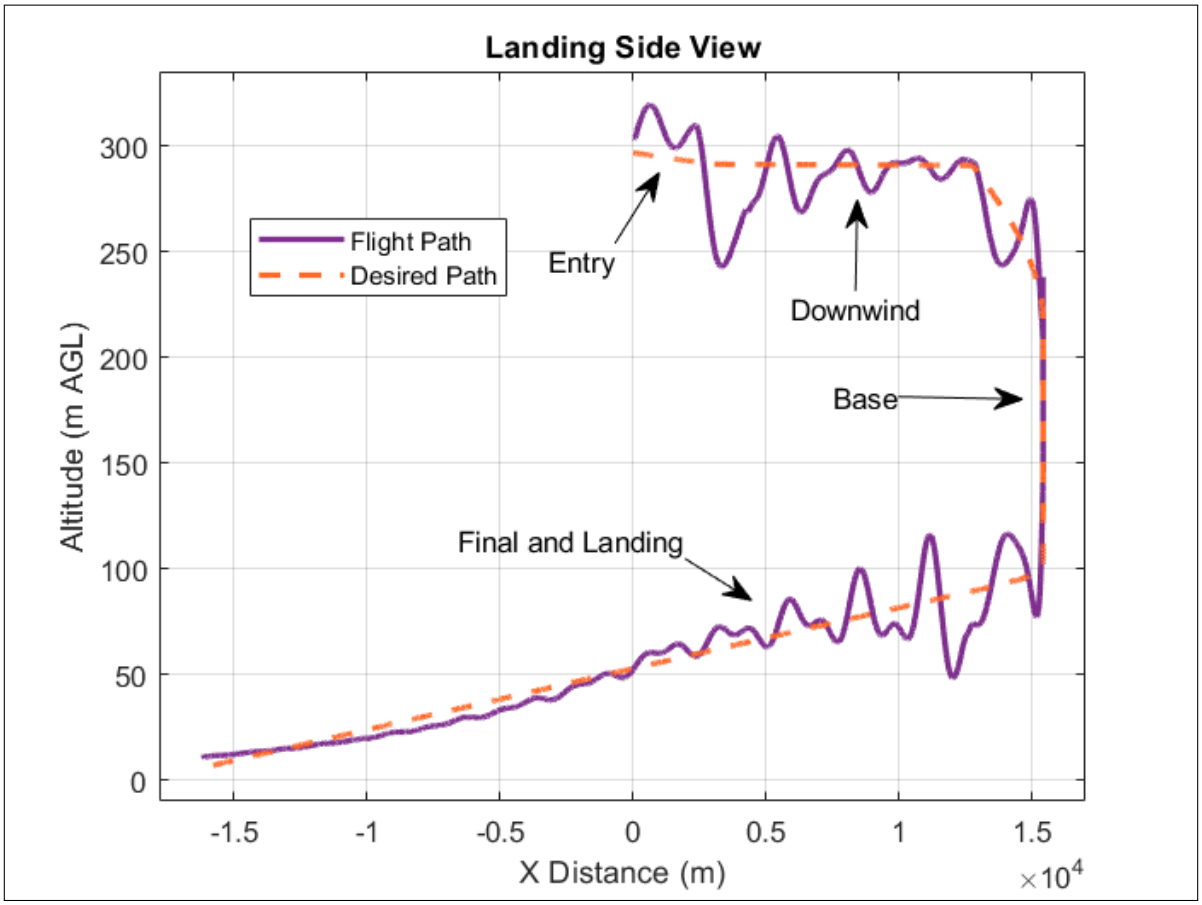

Figure 7.2 – Landing Side View. (X,Z) Altitude Plane

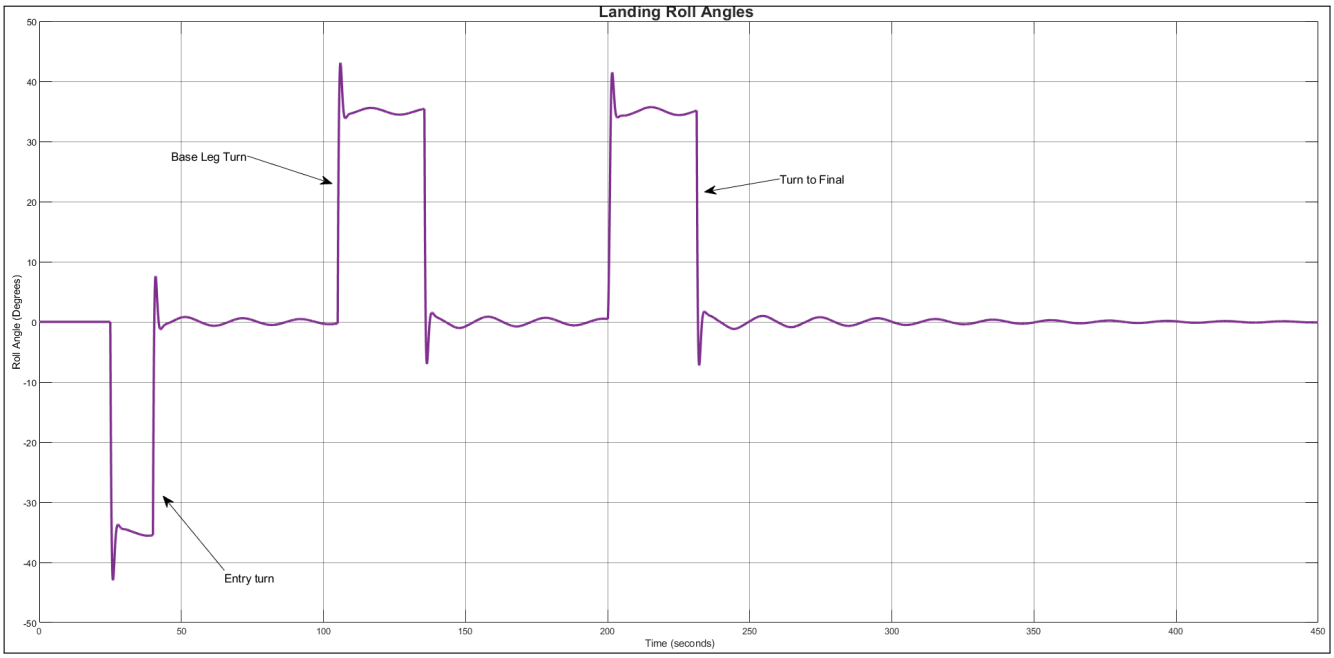

Figure 7.3 – Landing Roll Angles

8 Risk Analysis

The success of this project depends on meeting the performance metrics and thereby achieving the goals mentioned in the mission statement. Risk assessment assures the stakeholders, engineers and customers whether the plane is on track to be safe, hazard free, secure, and feasible for commercial use. It is impossible to avoid risks completely. However they can be prevented and mitigated ahead of time via risk analysis. In the time frame of product development, engineers usually have a way of anticipating the risks and accepting the technological risks encountered to a certain degree [6].

The team has provided a risk assessment definition in Table 8.1 based on the resources provided by Department of Defense [1], NASA Safety Measure [4], and United States Air force [3]. These sources provide the basic guideline to help assessing the risks and provide some mitigation mechanisms. They are divided in to two sections: Probability and Severity. Probability is the likelihood of risk to occur, while severity is the effect of the risk. To determine the risk assessments a color grading scale is provided in Table 8.2. Since this plane is a model only (no actual testing), the risks are mostly catered to the overall qualitative risk control. The risks anticipated column are color graded based on probability of that hazard occurring. Red colored risks will hinder all types of operation and may lead to complete failure of the mission. Light yellow/green are less likely to occur and thus may be accepted depending on the safety assessment. The values are assigned based on that specific risk severity.(i.e. 1 is catastrophic while 4 is negligible).

Table 8.1 – Risk Definitions

Risk Probability	Description
Frequent (**A**)	Often occurs, and is consistent threat to mission.
Probable (**B**)	Will occur several times in the life of an item
Occasional (**C**)	Likely to occur in the life span.
Remote (**D**)	Unlikely but Possible.
Improbable (**E**)	Highly unlikely to occur.
Eliminated (**F**)	Incapable of occurrence.
Risk Severity	**Description**
Catastrophic (**1**)	Could result in complete mission failure. death, irreversible impact.
Critical (**2**)	Results in partial disability, injuries, environmental impact, or monetary loss.
Marginal (**3**)	Injury or occupational illness for one or more lost work, moderate env-impact.
Negligible (**4**)	Injury or occupational illness not resulting in a lost work, minimal env-impact.

Table 8.2 – IMT-22 Anticipated Qualitative Risk Grading

	Risk Severity				
Risk Probability		Catastrophic (1)	Major (2)	Minor (3)	Negligible (4)
	Frequent (A)	A1	A2	A3	A4
	Probable (B)	B1	B2	B3	B4
	Improbable (E)	E1	E2	E3	E4

8.1 Risk Control and Assessment

The IMT-22 airplane is designed by taking the main anticipated risks in to account. The components are designed and selected in a manner they can mitigate and avoid the potential risks listed in Table 8.3. The risks are divided in to three sections. The Pre-flight (conceptual design, modeling and testing) phase, Post-flight phase (after landing), and In-flight phase (operation and performance). For a potential risk hazard, mitigation solutions were incorporated based on FAA Part 25 [2] and NTSB Safety Measures [5]. Although there are no perfect solutions, mitigation measures seek to lessen the impact of foreseen risks should they arise.

Table 8.3 – IMT-22 Risk Assessment

Hazard	Assessment	Risk	Mitigation
Pre Flight (testing, maintenance, simulation)			
Operational Cost	B2	Delayed project timeline	Clarified method on fund acquisition & allocation
System Design (Manufacturing Delays)	A4	Hinder project timeline, and delivery	Controlled and designated resource - allocation. Supply chain reorganization.
Faulty component	B1	Fatal crash, death, serious environmental impact	Pre-certification testing, and routine maintenance
Technological Limitation	B4	Does not meet the 2035 entry	Active research and development, modular design
In Flight (live operation and performance)			
Electrical, Fuel, or Hydraulic issue	B1	May cause fatal crash or hull loss	Redundant systems, proper insulation and compartmentalizing
Thermal (Fire) Issues	B3	Engine, Electrical, Mechanical	Double wall bumpers, electrical insulation and gaps, battery fire-suppression system.
Foreign Airplanes	E1	Mid air collision, causing fatal crash	Active tracking of other airplanes, instrumentation
Descend Flight (landing, taxi)			
Possible Engine Failure	B1	Crash landing, Environmental damage, Fire	Fully battery power for 30 minutes Single engine capability with glide up to 32 miles.
Vibrational Wear	B3	Structural and payload damage	Incorporate force damping measures, distribute static loads, preventative maintenance.
Control Burnout	B4	Minor effects on landing performance	Provide engineered stall warning Pilot stick shake feedback Proper signs and warning alerts.

9 Conclusion

As shown on the Simulink and performance simulations, the IMT-22 achieves all the the desired results. The aircraft can glide up to 32 miles, climb up to a rate of 709 ft/minute at 70% max thrust and can land with one or no engine. The fuel efficiency target was met and exceeded by 7%. The aircraft is also ICAO class C compliant and FAA Part 125 B and C certified. It can carry 54 passengers with luggage including crew, and takes off in under 2500 ft which is 2000 ft less than the required. The plane also exceeds the minimum cruise speed of 275 knots with a cruise speed of 350 knots (180 m/s), in addition to an additional 200 nautical miles of range over the required 1000 nautical miles.

Overall, the IMT-22 is a regional turboprop hybrid with an estimated 1200 nautical mile range, 52 passenger capacity, and 12660 pounds of passengers or cargo, all while reducing fuel usage by 27% when compared with current turboprop competitors. It is also reasonably priced and is expected to enter commercial service by 2035. Further efficiency gains may be found in future analysis through improved battery energy density, advanced composite techniques, and the addition of winglets to maximize the efficiency of the aircraft.

10 Appendix

10.1 Matlab Script for generating coefficients

```
%%%%%% Eyob Modded Lab-12 on 11_20 %%%%%%
% Read 5 XFLR5 data files for the crater_maker design

Datum = csvread('Datum.csv',7,0,[7 0 44 12]);
%Elevator increment data
Data_en3 = csvread('Datum-3.csv',7,0,[7 0 44 12]);
Data_en5 = csvread('Datum-5.csv',7,0,[7 0 44 12]);
Data_ep3 = csvread('Datum+3.csv',7,0,[7 0 44 12]);
Data_ep5 = csvread('Datum+5.csv',7,0,[7 0 44 12]);
%Rudder Increment data
Data_rn5 = csvread('Datum_Fin-5.csv',7,0,[7 0 44 12]);
Data_rn10 = csvread('Datum_Fin-10.csv',7,0,[7 0 44 12]);
Data_rp5 = csvread('Datum_Fin+5.csv',7,0,[7 0 44 12]);
Data_rp10 = csvread('Datum_Fin+10.csv',7,0,[7 0 44 12]);
%Aileron Increment data
Data_an5 = csvread('DatumAil-5.csv',7,0,[7 0 44 12]);
Data_an10 = csvread('DatumAil-10.csv',7,0,[7 0 44 12]);
Data_ap5 = csvread('DatumAil+5.csv',7,0,[7 0 44 12]);
Data_ap10 = csvread('DatumAil+10.csv',7,0,[7 0 44 12]);
%Beta Increment data
Data_bp3 = csvread('Datum_Beta+3.csv',7,0,[7 0 44 12]);
Data_bn3 = csvread('Datum_Beta-3.csv',7,0,[7 0 44 12]);
Data_bp6 = csvread('Datum_Beta+6.csv',7,0,[7 0 44 12]);
Data_bn6 = csvread('Datum_Beta-6.csv',7,0,[7 0 44 12]);

% datum values
alpha = Datum(:,1); % read angles of attack
% alpha = alpha(1:48);
CL_datum = Datum(:,3);
% CL_datum1 = CL_datum(1:38);
CD_datum = Datum(:,6);
% CD_datum1 = CD_datum(1:38);
Cm_datum = Datum(:,9);
% Cm_datum1 = Cm_datum(1:38);
```

```
CY_datum = Datum(:,7);
Cl_datum = Datum(:,8);
Cn_datum = Datum(:,10);

%% Elevator

% Create lift increment vectors for elev
dCL_en5 = Data_en5(:,3)- CL_datum;
dCL_ep3 = Data_ep3(:,3) - CL_datum;
dCL_e0 = CL_datum - CL_datum; % this vector will be all zeros
dCL_ep5 = Data_ep5(:,3) - CL_datum;
dCL_en3 = Data_en3(:,3) - CL_datum;

% Create drag increment vectors for elev
dCD_en5 = Data_en5(:,6)- CD_datum;
dCD_ep3 = Data_ep3(:,6) - CD_datum;
dCD_e0 = CD_datum - CD_datum; % this vector will be all zeros
dCD_ep5 = Data_ep5(:,6) - CD_datum;
dCD_en3 = Data_en3(:,6) - CD_datum;

% Create moment increment vectors for elev
dCm_en5 = Data_en5(:,9)- Cm_datum;
dCm_ep3 = Data_ep3(:,9) - Cm_datum;
dCm_e0 = Cm_datum - Cm_datum; % this vector will be all zeros
dCm_ep5 = Data_ep5(:,9) - Cm_datum;
dCm_en3 = Data_en3(:,9) - Cm_datum;

% Elevator deflection angle vector;
delev = [-5, -3, 0, 3, 5];

% Combine lift, drag, and moment coefficient increment vectors into a single increment arr
dCL_elev = [dCL_en5(1:38), dCL_en3(1:38), dCL_e0(1:38), dCL_ep3(1:38), dCL_ep5(1:38)];
dCD_elev = [dCD_en5(1:38), dCD_en3(1:38), dCD_e0(1:38), dCD_ep3(1:38), dCD_ep5(1:38)];
dCm_elev = [dCm_en5(1:38), dCm_en3(1:38), dCm_e0(1:38), dCm_ep3(1:38), dCm_ep5(1:38)];

% Save lift, drag, and moment coefficient increments to a .mat file
save('dCL_elev.mat', 'dCL_elev')
save('dCD_elev.mat', 'dCD_elev')
```

```
save('dCm_elev.mat', 'dCm_elev')

%% Rudder

% Create side force increment vectors for rudd
dCY_rn10 = Data_rn10(:,7) - CY_datum;
dCY_rn5 = Data_rn5(:,7) - CY_datum;
dCY_r0 = CY_datum - CY_datum; %Should be all zeros
dCY_rp5 = Data_rp5(:,7) - CY_datum;
dCY_rp10 = Data_rp10(:,7) - CY_datum;

% Create roll moment increment vectors for rudd
dCl_rn10 = Data_rn10(:,8) - Cl_datum;
dCl_rn5 = Data_rn5(:,8) - Cl_datum;
dCl_r0 = Cl_datum - Cl_datum; %Should be all zeros
dCl_rp5 = Data_rp5(:,8) - Cl_datum;
dCl_rp10 = Data_rp10(:,8) - Cl_datum;

% Create yaw moment increment vectors for rudd
dCn_rn10 = Data_rn10(:,10) - Cn_datum;
dCn_rn5 = Data_rn5(:,10) - Cn_datum;
dCn_r0 = Cn_datum - Cn_datum; %Should be all zeros
dCn_rp5 = Data_rp5(:,10) - Cn_datum;
dCn_rp10 = Data_rp10(:,10) - Cn_datum;

% Rudder deflection angle vector
drudder = [-10, -5, 0, 5, 10];

% Combine vectors into single array for each variable
dCY_rudder_alpha = [dCY_rn10(1:38), dCY_rn5(1:38), dCY_r0(1:38), dCY_rp5(1:38), dCY_rp10(1
dCl_rudder_alpha = [dCl_rn10(1:38), dCl_rn5(1:38), dCl_r0(1:38), dCl_rp5(1:38), dCl_rp10(1
dCn_rudder_alpha = [dCn_rn10(1:38), dCn_rn5(1:38), dCn_r0(1:38), dCn_rp5(1:38), dCn_rp10(1

% Save to a .mat file
save('dCY_rudder_alpha.mat', 'dCY_rudder_alpha')
save('dCl_rudder_alpha.mat', 'dCl_rudder_alpha')
save('dCn_rudder_alpha.mat', 'dCn_rudder_alpha')
```

```
%% Ailerons

% Create side force increment vectors for ailr
dCY_an10 = Data_an10(:,7) - CY_datum(1:38);
dCY_an5 = Data_an5(:,7) - CY_datum(1:38);
dCY_a0 = CY_datum - CY_datum; %Should be all zeros
dCY_ap5 = Data_ap5(:,7) - CY_datum(1:38);
dCY_ap10 = Data_ap10(:,7) - CY_datum(1:38);

% Create roll moment increment vectors for rudd
dCl_an10 = Data_an10(:,8) - Cl_datum(1:38);
dCl_an5 = Data_an5(:,8) - Cl_datum(1:38);
dCl_a0 = Cl_datum - Cl_datum; %Should be all zeros
dCl_ap5 = Data_ap5(:,8) - Cl_datum(1:38);
dCl_ap10 = Data_ap10(:,8) - Cl_datum(1:38);

% Create yaw moment increment vectors for rudd
dCn_an10 = Data_an10(:,10) - Cn_datum(1:38);
dCn_an5 = Data_an5(:,10) - Cn_datum(1:38);
dCn_a0 = Cn_datum - Cn_datum; %Should be all zeros
dCn_ap5 = Data_ap5(:,10) - Cn_datum(1:38);
dCn_ap10 = Data_ap10(:,10) - Cn_datum(1:38);

%Aileron deflection angle vector
daileron = [-10, -5, 0, 5, 10];

% Combine vectors into single array for each variable
dCY_aileron_alpha = [dCY_an10, dCY_an5(1:38), dCY_a0(1:38), dCY_ap5(1:38), dCY_ap10];
dCl_aileron_alpha = [dCl_an10, dCl_an5(1:38), dCl_a0(1:38), dCl_ap5(1:38), dCl_ap10];
dCn_aileron_alpha = [dCn_an10, dCn_an5(1:38), dCn_a0(1:38), dCn_ap5(1:38), dCn_ap10];

% Save to a .mat file
save('dCY_aileron_alpha.mat', 'dCY_aileron_alpha')
save('dCl_aileron_alpha.mat', 'dCl_aileron_alpha')
save('dCn_aileron_alpha.mat', 'dCn_aileron_alpha')


%% Beta
```

```
% Create side force increment vectors for beta
dCY_bn6 = Data_bn6(:,7) - CY_datum(1:38);
dCY_bn3 = Data_bn3(:,7) - CY_datum(1:38);
dCY_b0 = CY_datum - CY_datum; %Should be all zeros
dCY_bp3 = Data_bp3(:,7) - CY_datum(1:38);
dCY_bp6 = Data_bp6(:,7) - CY_datum(1:38);

% Create roll moment increment vectors for beta
dCl_bn6 = Data_bn6(:,8) - Cl_datum(1:38);
dCl_bn3 = Data_bn3(:,8) - Cl_datum(1:38);
dCl_b0 = Cl_datum - Cl_datum; %Should be all zeros
dCl_bp3 = Data_bp3(:,8) - Cl_datum(1:38);
dCl_bp6 = Data_bp6(:,8) - Cl_datum(1:38);

% Create yaw moment increment vectors for beta
dCn_bn6 = Data_bn6(:,10) - Cn_datum(1:38);
dCn_bn3 = Data_bn3(:,10) - Cn_datum(1:38);
dCn_b0 = Cn_datum - Cn_datum; %Should be all zeros
dCn_bp3 = Data_bp3(:,10) - Cn_datum(1:38);
dCn_bp6 = Data_bp6(:,10) - Cn_datum(1:38);

% Sideslip angle increment vector
dbeta = [-6, -3, 0, 3, 6];

% Combine vectors into single array for each variable
dCY_beta_alpha = [dCY_bn6(1:38), dCY_bn3(1:38), dCY_b0(1:38), dCY_bp3(1:38), dCY_bp6(1:38)
dCl_beta_alpha = [dCl_bn6(1:38), dCl_bn3(1:38), dCl_b0(1:38), dCl_bp3(1:38), dCl_bp6(1:38)
dCn_beta_alpha = [dCn_bn6(1:38), dCn_bn3(1:38), dCn_b0(1:38), dCn_bp3(1:38), dCn_bp6(1:38)

% Save to a .mat file
save('dCY_beta_alpha.mat', 'dCY_beta_alpha')
save('dCl_beta_alpha.mat', 'dCl_beta_alpha')
save('dCn_beta_alpha.mat', 'dCn_beta_alpha')
```

10.2 Matlab Script for Plotting Graphs

```
figure(1)
plot(alpha, CL_datum,'b', LineWidth=2)
xlabel('\alpha (deg)')
ylabel('CL')
title('CL_{Datum} vs Alpha')
grid on
% legend('Cn_{-6}','Cn_{-3}', 'Cn_{datum}','Cn_{+3}', 'Cn_{+6}')

figure(2)
plot(alpha, CD_datum,'m', LineWidth=2)
xlabel('\alpha (deg)')
ylabel('CD')
title('CD_{Datum} vs Alpha')
grid on

figure(3)
plot(alpha, Cm_datum,'r', LineWidth=2)
xlabel('\alpha (deg)')
ylabel('CM')
title('CM_{Datum} vs Alpha')
grid on

figure(4)
plot(alpha, dCL_elev,'r', LineWidth=2)
xlabel('\alpha (deg)','fontweight','bold')
ylabel('CL','fontweight','bold')
title('CL vs Alpha for Elevator')
legend('-5 deg','-3 deg', '0 deg','+3 deg', '+5 deg','Location','south','Orientation','hor
grid on

figure(5)
plot(alpha, dCL_elev,'r', LineWidth=2)
xlabel('\alpha (deg)','fontweight','bold')
ylabel('CL','fontweight','bold')
title('CL vs Alpha for Elevator')
legend('-5 deg','-3 deg', '0 deg','+3 deg', '+5 deg','Location','south','Orientation','hor
```

```
grid on

figure(6)
plot(alpha, dCL_elev,'r', LineWidth=2)
xlabel('\alpha (deg)','fontweight','bold')
ylabel('CL','fontweight','bold')
title('CL vs Alpha for Elevator')
legend('-5 deg','-3 deg', '0 deg','+3 deg', '+5 deg','Location','south','Orientation','hor
grid on
```

References

[1] Department of Defense. "Department of defense standard practice". In: *Mil-Std-882E* May (2008).

[2] FAA. "FAA PART-25 AIRWORTHINESS STANDARDS: TRANSPORT CATEGORY AIRPLANES". In: *Federal Aviation Administration* 7 (2021), pp. 195–470.

[3] Wright-patterson Force. "USAF Center of Excellence for Airworthiness". In: *AIR Ohio, Base* (2019), pp. 4–5.

[4] NASA. "NASA Strategic Plan 2014". In: *Nasa* (2014), pp. 1–68. URL: https://www.nasa.gov/image-feature/us-flag-in-the-cupola.

[5] NTSB-SS-05/01. "Risk Factors Associated with Weather-Related General Aviation Accidents". In: *National Transportation Safety Board* (2005).

[6] Daniel Raymer. "Aircraft Design: A Conceptual Approach, Sixth Edition". In: *Aircraft Design: A Conceptual Approach, Sixth Edition* (2018). DOI: 10.2514/4.104909.

[7] Thomas R. Yechout. "Aircraft Flight Mechanics: Performance, Static Stability, Dynamic Stability". In: *AIAA* (2014). URL: https://www.ptonline.com/articles/how-to-get-better-mfi-results.

[8] Nichols Ziegler. "Optimum Settings for Automatic Controllers". In: *ASME* (1942). URL: http://www.mstarlabs.com/control/znrule.html.